https://doi.org/10.5194/egusphere-2025-293
Preprint. Discussion started: 18 February 2025

The historical climate trend resulted in changed convective transport patterns in model simulations

Adrienne Jeske[1] and Holger Tost[1]

[1]Institute for Atmospheric Physics, Johannes Gutenberg-University Mainz

Correspondence: Adrienne Jeske (adjeske@uni-mainz.de)

Abstract. Convective transport leads to a rapid vertical redistribution of tracers. This has a major influence on the composition of the upper troposphere, a highly climate sensitive region. It is not yet clear how the convective transport is affected by climate change. In this study, we applied a new tool, the so-called convective exchange matrix, in historical simulations with the EMAC (ECHAM/MESSy Atmospheric Chemistry) chemistry-climate model to investigate the trends in convective transport. The simulated deep convection is penetrating higher but occurs less frequently from 2011 to 2020 than from 1980 to 1989. The increase in the vertical extend of convection is highly correlated to a rise in the tropopause height. Overall, convection transports material less efficient to the upper troposphere, but the transport directly into the tropopause region has on average increased from 2011 to 2020 in comparison to the 1980ies. These findings give rise for new opportunities to investigate long term simulations performed by EMAC with regard to the effects of convective transport. Further, they might provide a first insight into the trends of atmospheric convective transport due to changing atmospheric conditions and might serve as an estimate for the convective feedback to climate change.

1 Introduction

Moist convection plays a key role for the transport of heat and water in the Earth's atmosphere (Emanuel, 1994). Beyond that, deep convection is associated with extremely large vertical wind velocities. These lead to rapid vertical transport time scales and therefore, to a major redistribution of atmospheric tracers (Feichter and Crutzen, 1990). Consequently, convective transport has complex implications for the atmospheric composition and chemistry, especially in the upper troposphere (Mari et al., 2000; Lawrence et al., 2003; Bozem et al., 2017) . As some studies argue, deep convection even influences the composition of the lower stratosphere (Ray et al., 2004; Tinney and Homeyer, 2021; Gordon et al., 2024) and could lead to a downward transport of ozone rich air from the stratosphere to the upper troposphere (Frey et al., 2015).

Because it is highly important to capture convective transport and its effects (Barth et al., 2007), many efforts were made towards a better representation of convective transport in models (Mahowald et al., 1995; Lawrence and Rasch, 2005; Tost et al., 2010; Li et al., 2018), a more comprehensive understanding of this process (Doherty et al., 2005; Lawrence and Salzmann,

https://doi.org/10.5194/egusphere-2025-293
Preprint. Discussion started: 18 February 2025

2008; Bardakov et al., 2022) and the interplay of convective transport and the related scavenging (Mari et al., 2000; Barth et al., 2007; Bozem et al., 2017; Cuchiara et al., 2020, 2023). However it is not known yet, how convective transport will adapt to climate change.

Despite the transport effects, it is a hot topic in literature, how convection has changed and will change due to the extensive changes in our climate system we are facing. Lepore et al. (2021) found with the help of CMIP6 (Coupled Model Intercomparison Project Phase 6, Eyring et al. 2016) simulation data that in a warmer climate CAPE (convective available potential energy) increases, likely causing an enhancement in severe storm frequency. Del Genio et al. (2007) performed simulations with doubled CO2 concentrations and detected an increase in the updraft velocity in this case.

If the convection occurrence or strength of convection changes, it can be assumed that the convective transport will be modified as well. Stevenson et al. (2005) performed a 40 year projection to investigate the trends of tropospheric ozone concentrations under climate warming conditions. Thereby, O_3 is directly affected by convective transport itself and of its precursors as well as lightning NO_x emissions in deep convective cells (Stevenson et al., 2005). Within this simulation, the tropical convection occurs less frequently in the 2020s compared to the 1990s but the updrafts strengthened at about 150 hPa which influences the vertical transport. Stevenson et al. (2005) found, that the changes in the convective properties lead to a decrease in the column ozone, what implies a negative chemistry-climate feedback according to the authors.

The work by Stevenson et al. (2005) highlights the importance to investigate the adaptations of convective transport to understand the response of the climate system to warming. However, so far it is not fully clear, how convective transport processes change in detail and to which extent. Therefore, this study follows up with the question: How does climate change specifically influences the convective transport, i.e., the transport efficiency by the updraft, the downdraft and the large-scale subsidence and the vertical extend of these transport processes?

This manuscript addresses this question by performing historical simulations with the chemistry-climate model EMAC (ECHAM / MESSy Atmospheric Chemistry, Jöckel et al., 2006, 2010, 2016) using the convective transport scheme CVTRANS (ConVective tracer TRANSport) by Tost et al. (2010). To do so, we improved the representation of the turbulent detrainment and entrainment in CVTRANS and added a new feature to analyse convective transport, namely the convective exchange matrix. This new tool connects the convective transport from all possible starting levels to all possible destination levels in a model when utilising a convection parameterisation. This enables a deeper understanding of the changing transport processes and their causes. The focus of this study lies on the changes in the deep convective transport towards the upper troposphere over the past decades.

This study is structured as follows: The global chemistry climate model EMAC and submodel CVTRANS are described briefly in Sec. 2. In the same section, we introduce the adaptations and added features within the new version of CVTRANS. The simulation setup is described in Sec. 2.2. In Sec. 3, we analyse the results focusing on the changes in transport over the past decades. The implications, significance and the limitations are discussed in Sec. 4. The summary and the outlook are given in Sec. 5.

https://doi.org/10.5194/egusphere-2025-293
Preprint. Discussion started: 18 February 2025

2 Model description

2.1 EMAC

The global chemistry and climate model EMAC (Jöckel et al., 2006, 2010, 2016) consists of the general circulation model ECHAM5 (European Centre Hamburg general circulation model version 5, Roeckner et al., 2006) and the Modular Earth Submodel System (MESSy, Jöckel, 2006; Jöckel et al., 2010, 2016). MESSy is an interface to couple different submodels with a chosen base model and includes a steadily growing number of these submodels. For example, Vella et al. (2023) used EMAC recently to combine a global dynamic vegetation model with an atmospheric model. In this study, MESSy version 2.55 is used to link the submodel CVTRANS (Tost et al., 2010) with ECHAM. The dynamic representation of convection is given by the Tiedtke-Nordeng convection scheme (Tiedtke, 1989; Nordeng, 1994), as implemented in the CONVECT submodel within the MESSy structure (Tost et al., 2006).

2.2 Simulation setup

A three dimensional global simulation has been conducted with the convective exchange matrix implemented utilising the chemistry climate model EMAC (Jöckel et al., 2010, 2016). 31 vertical pressure level up to 10 Pa are used and a horizontal resolution of T63 (triangular truncation with wavenumber 63) has been applied. This is associated with 192 $\times$ 96 gridpoints and a time step of 12 min. The simulation period spans the time from the beginning of 1979 until the end of 2020.

Temperature, vorticity, divergence, surface pressure, sea surface temperature and sea ice consentrations are nudged towards ECMWF Reanalysis fifth generation (ERA5, Hersbach et al., 2020). The nudging is based on Jeuken et al. (1996) and applied as described by Jöckel et al. (2006). A basic methane chemistry is applied to take the water vapour production in the stratosphere and its influence on radiation into account using the submodel CH4 (Winterstein and Jöckel, 2021). Further considerations of chemical reactions are not necessary, because this study exclusively investigates the redistribution of air masses by convection and not the effect on single tracers. Monthly mean values for greenhouse gases are used to include their radiative effect based on Jöckel et al. (2016). The Tanre et al. (1984) climatology is used for tropospheric aerosol as described by Jöckel et al. (2016). For the stratospheric aerosol radiative effect optical properties of the CCMI (Chemistry–Climate Model Initiative) database (Revell et al., 2017) are applied, e.g., as in Jöckel et al. (2016).

The simulations have been performed at the national super computing system Mogon NHR (Nationales Hochleistunggsrechnen). The computing time tests have been conducted at Levante at the German Climate Computing Centre (DKRZ, Deutsches Klimarechenzentrum).

2.3 CVTRANS

The submodel CVTRANS (ConVective tracer TRANSport) was introduced by Tost et al. (2010) to account for convective tracer transport in EMAC. It makes use of a single plume / bulk convection parameterisation based on the formulation of Lawrence and Rasch (2005). Tost et al. (2010) applied the convective mass fluxes for the updraft, downdraft, entrainment and

https://doi.org/10.5194/egusphere-2025-293
Preprint. Discussion started: 18 February 2025

detrainment from the convection parameterisation to calculate the redistribution of the tracers. The mass fluxes must fulfil the following equations

$$F_{\mathrm{u}}^{k} = F_{\mathrm{u}}^{k+1} + E_{\mathrm{u}}^{k} + D_{\mathrm{u}}^{k} \tag{1a}$$

$$F_{\mathrm{d}}^{k+1} = F_{\mathrm{d}}^{k} + E_{\mathrm{d}}^{k} + D_{\mathrm{d}}^{k} \tag{1b}$$

as described by Tost et al. (2010) with F referring to the mass fluxes, D the detrainment and E the entrainment. The subscripts $_{\mathrm{u}}$ and $_{\mathrm{d}}$ denote the updraft and the downdraft. k indicates the model level. If this relation is not satisfied, the detrainment or entrainment should be adapted accordingly (Tost et al., 2010).

Strong updrafts can lead to mass balance problems, i.e., more mass is transported out of a model box as mass is transported into the box in one time step. The mass fluxes are re-scaled in such cases to prevent a mass imbalance. This procedure can lead to a damping of the convective transport. To overcome this issue, Ouwersloot et al. (2015) included intermediate time stepping in CVTRANS to ensure an optimum handling of very strong convective events.

Note, that the transport of water vapor and hydrometeors is not considered in the convective tracer transport algorithm, as the convection parameterisation itself takes care of the redistribution of water species.

2.4 Modifications of CVTRANS

2.4.1 Revision of the closure formulation in the CVTRANS submodule

Following Tiedtke (1989), the detrainment and the entrainment are given by an organised and a turbulent driven component. This is equally valid for the downdraft and the updraft. In the Tiedtke-Nordeng scheme the same approach is made (Nordeng, 1994).

In the former versions of CVTRANS by Tost et al. (2010) and Ouwersloot et al. (2015), it could happen in some cases that the formulation of the closure eliminated the entrainment and detrainment due to turbulence. To fulfill Eq. 1, the situation could arise that the entrainment had to be set to zero to calculate a closed mass balance; however, this would also erroneously eliminate the turbulent entrainment, which is always active in rapidly ascending or descending air masses. The entrainment rate is given by

$$E_{\mathrm{u}}^{k} = F_{\mathrm{u}}^{k} - F_{\mathrm{u}}^{k+1} + D_{\mathrm{u}}^{k}, \tag{2}$$

as long as the updraft mass flux leaving the box at its top is larger than the incoming updraft mass flux from below. All quantities are positive by definition.

If instead the incoming updraft mass flux is larger than the mass flux leaving the box at the top, the detrainment will be recalculated with the help of the closure as follows

$$D_{\mathrm{u}}^{k} = F_{\mathrm{u}}^{k+1} - F_{\mathrm{u}}^{k} + E_{\mathrm{u}}^{k}. \tag{3}$$

https://doi.org/10.5194/egusphere-2025-293
Preprint. Discussion started: 18 February 2025

If both equations for entrainment and detrainment are properly solved, no turbulent detainment or entertainment is accidentally set to zero. The same approach is taken for the downdraft.

A formulation following Tiedtke (1989) for the turbulent mixing is embedded to ensure the existence of turbulent entrainment and detrainment in updrafts and downdrafts in the closure part, which corrects potentially erroneous zero turbulent events. The adaptive time stepping by Ouwersloot et al. (2015) must be applied, otherwise, the calculation of the air mass transport can lead to negative values or a cutting of the strength of the mass fluxes. Both consequences are not desirable. Hence, we argue that adaptive time stepping should be applied in every simulation using CVTRANS.

2.4.2 Detrainment of entrained air in the downdraft

In CVTRANS, the parameter f_{det} gives the portion of material that is detrained directly after the entrainment in the same box as described by Ouwersloot et al. (2015). f_{det} is only computed and applied for the calculations concerning the updraft detrainment. Taking turbulence into account, we need to adapt equation 2 from Ouwersloot et al. (2015) also for the downdraft:

$$C^k_{\mathrm{d,det}} = \frac{(D^k_{\mathrm{d}} - f_{\mathrm{det}} E^k_{\mathrm{d}}) C^k_{\mathrm{d}} + f_{\mathrm{det}} E^k_{\mathrm{d}} C^k_{\mathrm{env}}}{D^k_{\mathrm{d}}}. \tag{4}$$

2.4.3 Description of the convective exchange matrix

The convective exchange matrix builds upon the concept of CVTRANS. First, in every vertical model level $(1, 2, ..., N)$ one pseudo tracer $(\boldsymbol{P_1}, \boldsymbol{P_2}, ..., \boldsymbol{P_N})$ is initialised with a value of 1 kg m^{-2}. N denotes the number of model levels. In all other levels the pseudo tracers are equal to zero. The vertical profiles of the pseudo tracers can be written as N dimensional vectors. Applying this, the pseudo tracer $\boldsymbol{P_1}$ is given by $\boldsymbol{P_1} = (1, 0, 0, ..., 0)$ and $\boldsymbol{P_2}$ is $\boldsymbol{P_2} = (0, 1, 0, ..., 0)$. Putting all these vectors together results in an $N \times N$ diagonal matrix as can be seen on the left side of Fig. 1(a).

The time integration, i.e., the vertical redistribution by convective transport of the pseudo tracer field, is performed based on CVTRANS. This results in the convective exchange matrix ($\mathbf{TrMa}$). The entries of the matrix give the portion of the air mass (m_{air}) that was transported from a specific level (given by the pseudo tracer field in the beginning) to a certain departure level. For example, $\mathbf{TrMa}_{i,j}$ with $i, j = 1, ..., N$ describes how much m_{air} was transported from level i to level j. Is $j = i$, then $\mathbf{TrMa}_{i,i}$ characterise the contribution of level i to level i itself. In other words, it shows the amount of air that was not affected during the convective event. This is illustrated in Fig. 1(b) highlighted in red. The upper left entries (yellow in Fig. 1) represent the transport from a level i to level j with i > j, i.e. the upward transport to level j which started in level i. Thereby, the notation is that the lowest model level has the highest number and the uppermost level is level 1. The downward transport (transport from a lower level number to a higher level number in this notation) is marked by the blue colour in Fig. 1(b). The illustration Fig. S1 in the electronically supplements can be used as guideline for the interpretation of the convective exchange matrix.

The redistributed concentrations of trace species can be calculated with the convective exchange matrix by a simple matrix multiplication of the TrMa with the vertical tracer mixing ratio profile, as now implemented in CVTRANS v3.0. For a small

https://doi.org/10.5194/egusphere-2025-293
Preprint. Discussion started: 18 February 2025

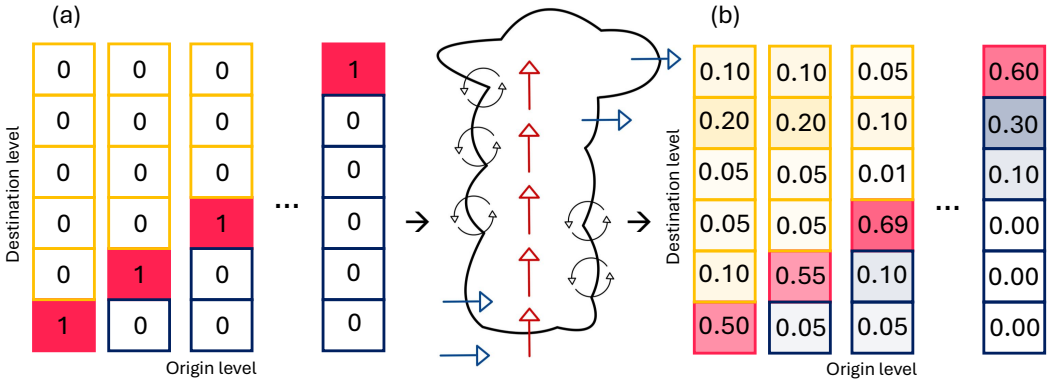

Figure 1. Sketch of the principle behind the convective exchange matrix. (a) shows the input matrix that is redistributed by convective transport processes. The redistribution is calculated with the submodule CVTRANS. The red arrows indicate the updraft mass flux, the blue ones the organised detraning and entraining and the thin black ones the turbulent mixing. The convective exchange matrix is a result of the interplay of updraft, downdraft, large-scale subsidence, entrainment and detrainment from/into up- and downdraft, but, for simplicity, only the updraft related processes are shown in this sketch. Panel (b) shows an example of a convective exchange matrix. (b) is only for illustration and not a real case calculated during a simulation. In both matrices, the reddish coloured fields denote the main diagonal. The yellow fields shows the matrix entries influenced by the updraft and the blue fields denote the matrix entries affected by the downdraft and the large-scale subsidence.

number of tracers, the computational efficiency is similar when the convective exchange matrix is applied to calculate the new concentrations of the tracers after the convective transport instead of using the transport algorithm itself.

The advantage of the convective exchange matrix is that the effects of the tracer transport can be studied disentangled from the specific background profiles of the tracers. Thus, it can be investigated, e.g., where the maximum outflow height is located and how much air mass can be transported upward inside the undiluted core of the convective system. The contribution to a certain destination level can be calculated for all starting levels. This can be helpful to track a measured air mass containing tracers backward and to investigate how strongly it was affected by convection in its air mass history.

3 Results

In this section, the differences in the convective exchange matrix are investigated due to the adaptations in CVTRANS based on one example case. Afterwards, the convective exchange matrix is applied to study the effect of climate change on the convective transport. For the latter case, nudged historical simulations were performed.

https://doi.org/10.5194/egusphere-2025-293
Preprint. Discussion started: 18 February 2025

3.1 Intercomparison of the adaptations using the convective exchange matrix

We performed three simulations to demonstrate the effects of the described changes in the submodel CVTRANS. One simulation was made with CVTRANS modified as described in the Sec. 2.4.1 and 2.4.2 (CVTRANSnew). A second was derived for comparison applying the former default version of CVTRANS (CVTRANSold). The last one is similar to CVTRANSnew but with enhanced turbulent mixing (CVTRANSturb). Despite the Convective exchange matrix is a new feature in CVTRANS 3.0, this tool was implemented and turned on in all simulations. Thus, the convective exchange matrices can be compared for the different treatments of turbulent mixing.

Figure 2(a) shows the convective exchange matrix derived with CVTRANSold for one exemplary deep convective event. The convective transport does not influence a large portion of the air mass in many levels. This can be clearly seen on the main diagonal of the convective exchange matrix. The portion of air mass that stays in the same level ranges between 6.96% and 92.43% for all levels where convection is active. The large-scale subsidence is a strong, but also a slow process. Therefore, it has a significant impact on the diagonal below the main diagonal. The values are commonly in the same order of magnitude as in the box above. The descending portions are often even higher as the ones not affected by convection. For example, more than 90% of the air that was originally at 551.62 hPa (level 20) and subsided to 592.81 hPa (level 21).

The large-scale subsidence balances together with the downdraft the updraft in CVTRANS (Tost et al., 2010). The subsidence is formulated in such a way that it is much slower than the updraft. This is realised by allowing the subsidence to transport mass to the model level directly below the original level only (see Equation (2) from Tost et al., 2010). Therefore, this outstanding second diagonal can be seen in the convective exchange matrix in Fig. 2(a).

The upward transport is largest when starting from levels between the lowest level at 937.63 hPa and level 28 at 873.29 hPa compared to other origin levels. This indicates a huge boundary layer to mid and upper troposphere transport. The upward transport decreases with increasing height of the level of origin for many but not all levels monotonically (moving to the right for different origin levels on the x-axis for the same destination level, depicted on the y-axis). The upward transport to level 5 (90.06 hPa) makes up to almost 4 %. It is the strongest in the upper troposphere, suggesting that level 5 is the main outflow level of the convective system.

The transport is intermittent in Fig. 2(a). For example, no material is transported from level 31 (937.63 hPa) to level 29 (902.65 hPa) in spite of the transport from level 31 to levels above 838.82 hPa. The main organised entrainment is taking place in the region below 838.82 hPa and consequently the missing detrainment occurred due to the suppression of turbulent detainment as described above. Also the upward transport from the upper levels exhibits "missing values" due to a lack in entrainment in the upper levels, where the organised detrainment is emphasised. This error is corrected in the new version of CVTRANS. Consequently, the transport is continuous in Fig. 2(b).

The transport from level 937.63 hPa to 902.65 hPa is still small compared with the transport to the levels above 838.82 hPa. The turbulent detrainment of air in the boundary layer and lower troposphere has implications for the mid and upper troposphere, i.e., less material from the surface level will arrive in the mid and upper troposphere because it is partly detrained below (Fig. 3(a)). Only 3.13 % of the air mass from level 31 reaches the main outflow level.

https://doi.org/10.5194/egusphere-2025-293
Preprint. Discussion started: 18 February 2025

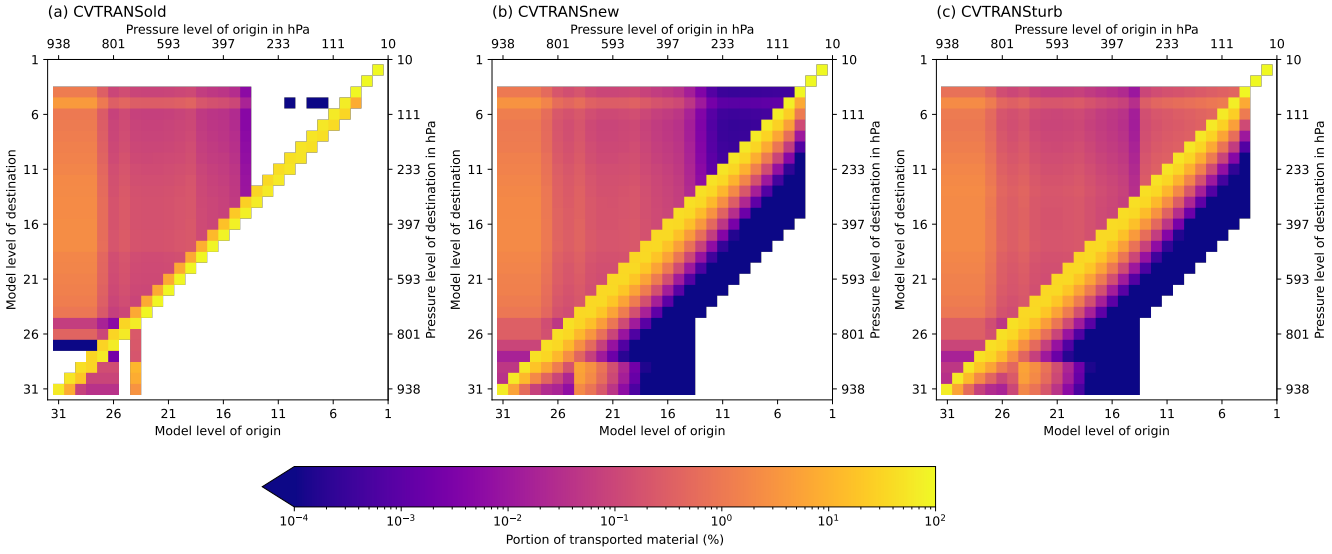

Figure 2. Convective exchange matrix for one specific event. The convective event was located over west Australia in south summer (23.316°S, 120.000°E on 1st January 1979 at 5 UTC). The convective exchange matrix is displayed for one time step. (a) shows the convective exchange matrix calculated with CVTRANSold, (b) the convective exchange matrix calculated with CVTRANSnew and (c) the convective exchange matrix as (b) but with enhanced turbulent mixing (CVTRANSturb).

Partly material is entrained in the updraft in the upper troposphere due to turbulent mixing. The transport portions clearly distinguish the new from the old CVTRANS version, but the values are small and therefore the quantitative impacts are barely noticeable. The downdraft is pronounced when CVTRANSnew is applied. Air mass is shifted to a greater extend by the downdraft to the lowermost three levels by CVTRANSnew (Fig. 2(b)) than by the old version of the convective tracer transport scheme (Fig. 2(a)).

The number of side diagonals below the main diagonal has increased comparing Fig. 2(a) with Fig. 2(b). This is can be attributed to the application of the adaptive time stepping according to Ouwersloot et al. (2015). Thereby, an algorithm chooses as many subtimesteps as necessary in order to avoid mass balancing issues instead of cutting the mass fluxes. The adaptive time stepping allows the convection, especially the updrafts to be as strong and as fast as they are given by the convection parameterisation. Consequently, the large-scale subsidence becomes elevated as well and can cover more then one vertical levels, i.e., as many levels as there are substeps required, as the re-distributed mass is calculated for each substep individually, including the large-scale subsidence in each grid cell. This leads to a more smeared signal of the large-scale subsidence in Fig. 2(b).

The same convective system is shown in Fig. 2(c) for high turbulent mixing. The turbulent mixing in this case is enhanced, i.e., it is as strong as the maximised turbulent mixing as suggested by Tiedtke (1989).

The difference in the upper troposphere is substantial when comparing to CVTRANSnew. A distinct larger fraction of material is entrained due to the enhanced turbulence in the upper troposphere into the updraft. Therefore, less material is

https://doi.org/10.5194/egusphere-2025-293
Preprint. Discussion started: 18 February 2025

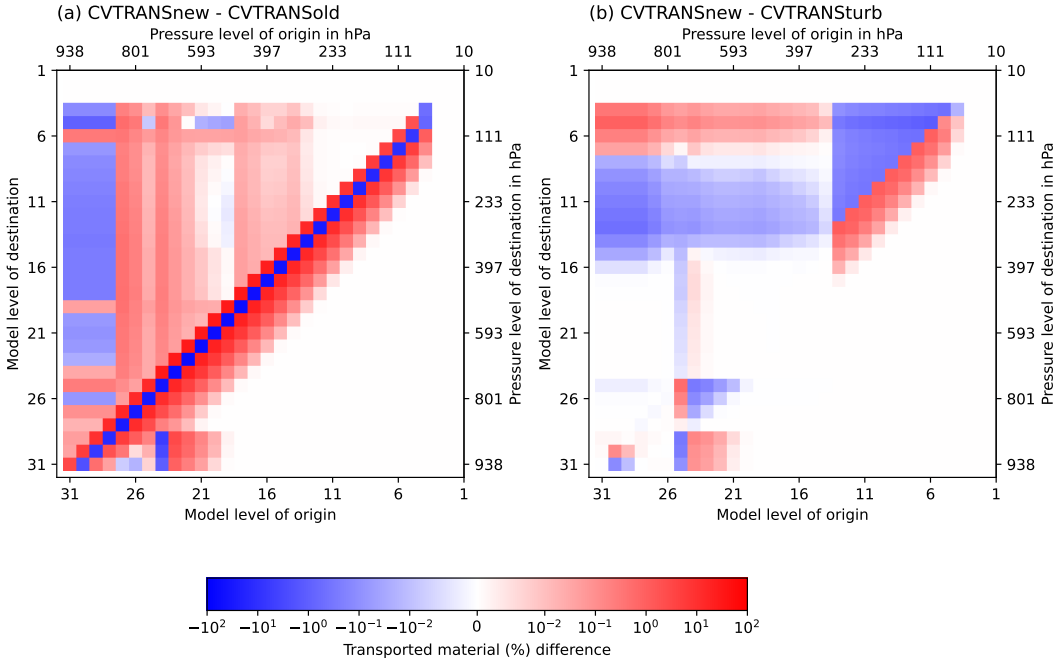

Figure 3. Difference (a) between the convective exchange matrix calculated with CVTRANSnew and the convective exchange matrix computed with CVTRANSold and (b) between the convective exchange matrix based on CVTRANSnew and the one calculated wit CV-TRANSturb.

directly transported from the boundary layer to the upper troposphere. The material is instead detrained already via mixing in the mid troposphere as can be seen in Fig. 3(b). It can be assumed given that bulk formulations tend to transport material less efficient to the upper troposphere as the more complex plume ensemble based approaches (Lawrence and Rasch, 2005) that the transport to the upper troposphere by CVTRANSturb is not efficient enough.

3.2 Convective transport trends

We performed nudged EMAC simulations including CVTRANS 3.0 starting in January 1979 to December 2020. Of this time period, the first year is excluded from the analysis to reduce spin-up effects. The convective properties and the convective transport are considered in the analysis for 1980 to 2020. This time period is sufficient to give a first impression about the climate response of the modelled convective transport since climate signals become recognisable on time scales of 30 years. The investigations are only performed between 60°S and 60°N because this is the area, where convection is of high relevance.

Remark: In the analysis, the transport is discussed referring to model levels and not pressure levels. This is due to the fact, that pressure varies largely between the boxes mainly due to orography and secondary due to weather systems. A re-gridding is not possible in a convincing manner, as interpolation artefacts would violate the mass balance and the mass redistribution.

https://doi.org/10.5194/egusphere-2025-293
Preprint. Discussion started: 18 February 2025

We try to refer to specific areas in the atmosphere as for example the UT or the mid troposphere for a better understanding, but please keep in mind that these areas vary as well with orography and furthermore with latitude.

3.2.1 Global changes

The convective transport matrix is shown in Fig. 4 for the temporal mean of the ten year period 2011 to 2020 and the area weighted mean between 60°N and 60°S. The mean transport matrix is shaped by a large number of initial unit matrices because atmospheric moist convection is a rather localised effect. As a consequence, the mean convective transport is of cause not as intense on a global scale as for a an individual local event (compare Fig. 2(a)). Nevertheless, the convective transport has a non-negligible effect on large scales.

The convective transport based on the Tiedtke-Nordeng convection parameterisation indicates typical features. The strongest upward transport starts in the lower free troposphere and in the boundary layer (level 31 to 26) and reaches not very far into the free troposphere (level 29 to 25), representing shallow convection and turbulent detrainment from updrafts. Deep upward transport starts mostly in the same area (levels 31 to 28), but shows lower fractions as the transport into the lower free troposphere. Higher starting levels are associated with lower portions of upward transported material.

The large-scale subsidence is obvious over two to three levels as the dominant downward transport mechanism below the main diagonal. Also the effects by downdrafts is striking. For the lower to mid tropospheric levels, the downdrafts lead to a clearly distinguishable increase in the transported mass portion to the lowest three model levels on a global scale.

Figure 5 shows the temporal and spatial mean convective transport compared between 2011 and 2020 to the reference period from 1980 to 1989. The transport to the upper levels increased significantly. The upward transport has strengthened to the level 4 to 7, the height of the tropical tropopause, from all starting levels below the destination levels. In the mid latitudes, these height levels are located in the stratosphere and are only occasionally influenced by deep convection. The large-scale subsidence adapted accordingly. More material descents from levels which are associated with the upper troposphere in the tropics and with the upper troposphere and lower stratosphere in the mid latitudes (between level 12 and 4).

These features of the difference convective exchange matrix (Fig. 5) can be explained considering the frequency distributions of the updraft mass fluxes compared for the reference time period and 2011 to 2020 (Fig. 6). In Fig. 6, the mass fluxes from deep convective events were categorised according to their strength. The lowest class (below 1×10^{-7} kg m^{-2} s^{-1}) contains all no events, so the cases where no deep convection occurred or the mass fluxes were to small. The class with the strongest updraft mass fluxes contains all mass fluxes which are stronger than 0.2 kg m^{-2} s^{-1}. This classification was performed for all height levels. The difference of these mass flux distributions is shown in Fig. 6 for a selected set of model levels and for the values from 2011 to 2020 minus the ones of 1980 to 1989. For a better visualisation the symmetric logarithmic difference is shown instead of the absolute numbers.

The updraft mass flux in the upper levels shifts to stronger mass fluxes in the later time period. Moreover, more events reaching up to higher levels from 2011 to 2020 in comparison to the reference period. This trend is consisted with the increased transport to the upper level as observed in Fig. 5.

https://doi.org/10.5194/egusphere-2025-293
Preprint. Discussion started: 18 February 2025

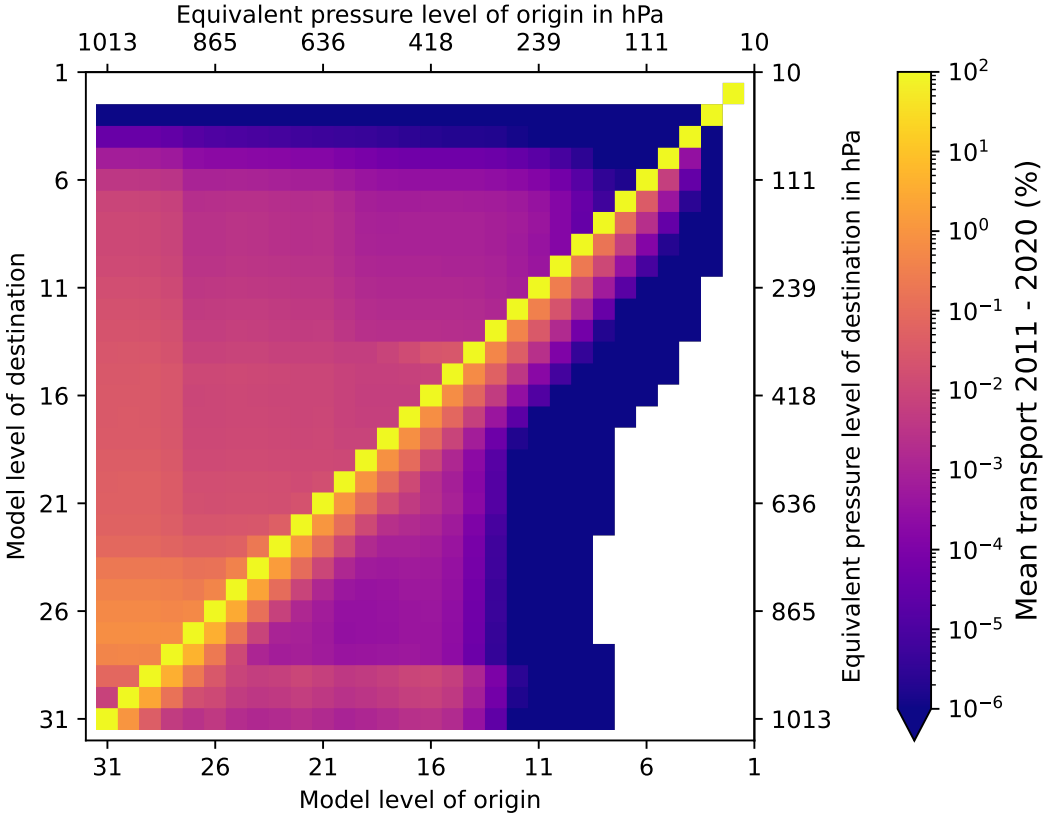

Figure 4. Area weighted between 60°N and 60°S and temporal mean convective transport matrix, i.e., the fraction of air mass which was transported from a origin to a source level, for 2011 to 2020. Note that the equivalent pressure (upper and right axis) is determined from a standard atmosphere over the ocean with zero orography.

The enhanced transport to higher levels could be explained by an increase in strength of the convection or even an enhancement of convection overshooting. A non-significant tendency towards more overshooting convection is predicted by the Tiedtke-Nordeng scheme over the 41 year time period. Thereby, overshooting is defined as events where the updraft mass flux reached beyond the tropopause in one column. It cannot be ruled out that the detected overshooting is only an artefact of the coarse model resolution because both, the tropopause height and the mass flux are mean values. It can be assumed that both quantities vary significantly within a box. However, the latter does not affect the convective transport in the model because the transport only sees the grid box mean values.

Wu et al. (2023) found an increasing trend in tropical overshooting convection based on simulations from 1979 to 2008 and based on satellite obeservations from 1998 to 2013. Concerning this study, convective tropopause overshooting can be ruled out as primary source for the major increased convective transport to the levels 7 to 4. The impacts of the overshooting on this trend are negligible due to the small and non-significant changes in overshooting in our simulation.

https://doi.org/10.5194/egusphere-2025-293
Preprint. Discussion started: 18 February 2025

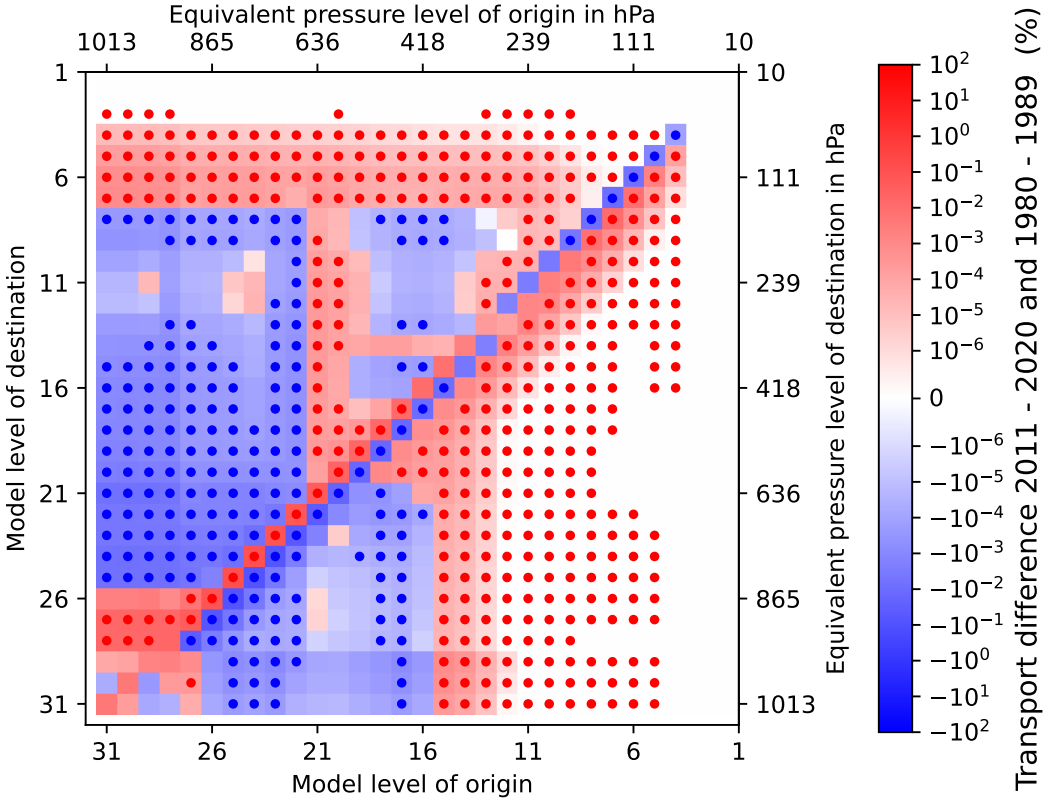

Figure 5. Changes in the convective mean transport between 60°S and 60°N. The temporal (ten year) and global (area weighted) convective exchange matrix is compared from 2011 to 2020 and from 1980 to 1989. Red colours denote that the values were higher in the period 2011 to 2020 and blue boxes show that the entry in the convective exchange matrix was higher from 1980 to 1989. A dot in a box indicates statistical significance. A two sided student t-test was used with a significance threshold of 1% for every side of the t-distribution.

The model predicts an increase in the global mean tropopause height (not shown). A higher troposphere could clear the path for convection with a larger vertical extend, but an increased penetration of convection could also cause a rise of the tropopause height. Deep convection tends to occur less frequent (Fig. 7) and for this reason the increased height of the deep convection has only rather locally an impact on the tropopause height. Therefore, we assume that the dominating process here is the change in tropopause height leading to deeper convection and not vice versa.

The upward transport has decreased from the starting levels between 31 to 21 to the destination levels in the mid troposphere and some upper tropospheric levels in the later time period (see Fig. 5). Fig. 6 is considered again to examine possible reasons for this decrease in upward transport. Less deep updraft convective mass fluxes are counted in the period from 2011 to 2020 in comparison to the 1980ies in many height levels with relevant values (larger 1×10^{-7} kg m^{-2} s^{-1}). However, a bimodal trend emerges from Fig. 6 in terms of the changes in the distribution of the deep updraft mass fluxes. The mass fluxes tend to be either at the stronger edge or very close to zero in the later time period. In level 6, higher mass fluxes are generally favoured in

https://doi.org/10.5194/egusphere-2025-293
Preprint. Discussion started: 18 February 2025

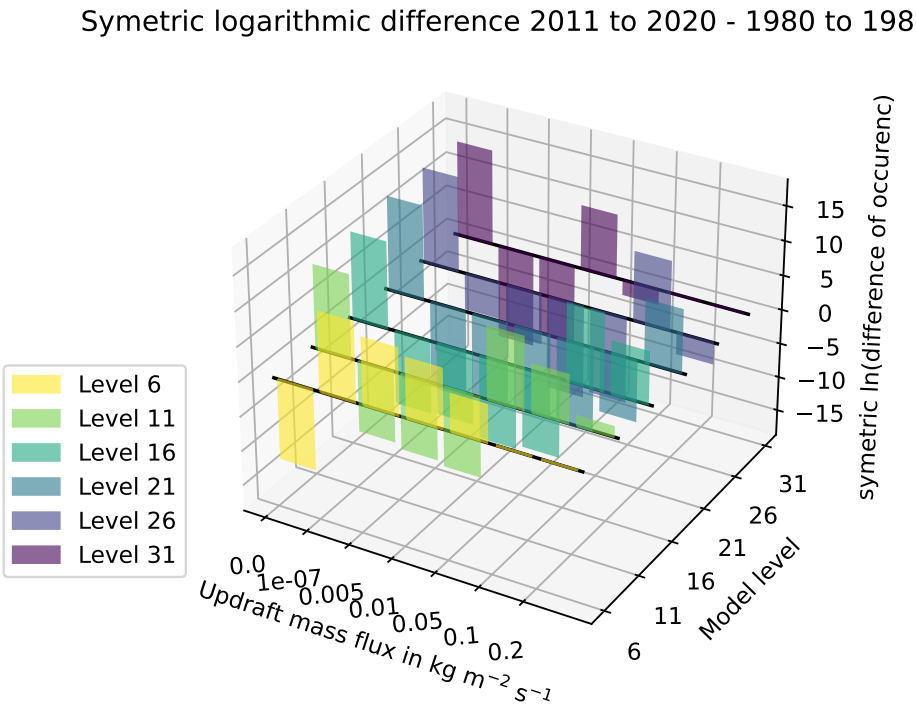

Figure 6. The distribution of the updraft mass fluxes is given as the symmetric logarithmic difference between the absolute frequency distributions of 2011 to 2020 and 1980 to 1989. The colors denote different altitude levels. Updraft mass fluxes are divided into seven categories. Updraft mass fluxes below 1×10^{-7} kg m^{-2} s^{-1} are not considered in the transport routine CVTRANS. Therefore, these mass fluxes are in the smallest category and are considered as no occurrence of convection.

the later period. Therefore, the negative trend in Fig. 5 can partly be attributed to an increase in the outflow height. In addition, a decreasing trend in the occurrence of deep convective events over the 41 year period is determined (Fig. 7).

The upward transport increased for the starting levels 20 and 21 depicted in Fig. 5. This leads to the hypothesis that mid level convection occurred more frequently in the later time period but the mid level convection according to the definition in the Tiedtke-Nordeng scheme did not increase in number (not shown). Therefore, an increase in the frequency of the midlevel convection can not be the reason, but the penetration height of the convection might. Not only the deep convection reaches higher in the later time period, but also the shallow convection. The shallow updraft mass fluxes tended to higher values in level 20 and level 21 (free troposphere). The same is the case for the midlevel convection. However, the midlevel convection headed towards a more frequent occurrence of the higher massfluxes for a wide range of altitude levels. These could play a role for this prominent increase of upward transport from two of the free tropospheric levels (level 21 and 20). Nevertheless, the cause cannot be conclusively clarified at this point.

https://doi.org/10.5194/egusphere-2025-293
Preprint. Discussion started: 18 February 2025

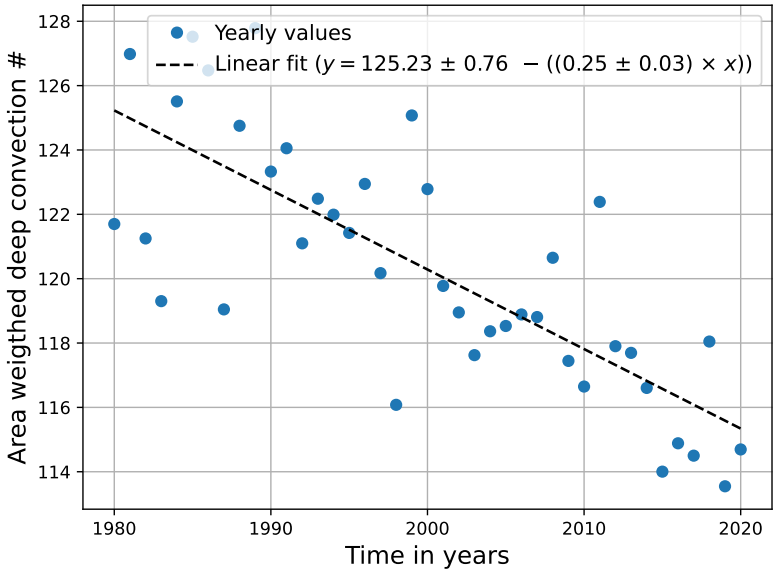

Figure 7. Normalised time development of the area weighted deep convection events per year. The crosses denote the yearly number of convective events and the dashed line is the linear fit of the area weighted deep convection events. x denotes the number of relative years, thus, x is equal zero for 1980. The standard error of the slope and the intercept are given for the linear fit. y is the number of area weighted deep convective events per year.

The downdrafts shift to higher starting levels (Fig. 5). On the one hand, the impact of downdrafts starting at levels 15 to 13 has increased in the later time period. On the other hand, the downward motion is reduced for origin levels between 26 and 16 (representing the free troposphere in the tropics and the upper troposphere in the higher latitudes) in case of the mean value from 2011 to 2020. This finding goes well along with the height increase of the deep convective systems.

A strengthening of the updraft detrainment is observed in Fig. 5 in the lower troposphere (up to level 26). This could be due to an increase in shallow convection because of the water vapor and lapse rate feedback on convection (e.g., Dagan et al., 2018, and references therein). However, the global occurrence of shallow convection did not significantly increase during the 41 year period (not shown). This means, that either the shallow convection intensifies or the detrainment of mid level and / or deep convection must increase.

In total, more material stays in its original level for levels in the boundary layer to mid troposphere. This trend is for many mid tropospheric levels (between level 17 and 27) significant. This also points towards an overall reduced deep convective transport.

https://doi.org/10.5194/egusphere-2025-293
Preprint. Discussion started: 18 February 2025

3.2.2 Zonal trends

In Fig. 8 the difference convective exchange matrix is shown for 30°N to 30°S. The convective transport increased to levels above level 7 from 2011 to 2020 in comparison to the 1980ies. The downdrafts shift as well to higher starting levels, and more large-scale subsidence is observed for the upper tropospheric to lower startospheric levels. As in the global case, more material stays in the starting level and is not affected by the convection for a huge number of levels. The convective transport increases compared to the reference period in the lowermost three levels. This is the only distinct difference between the tropical and the global trends. Overall, the trends in the tropics match well with the ones discussed for the global case.

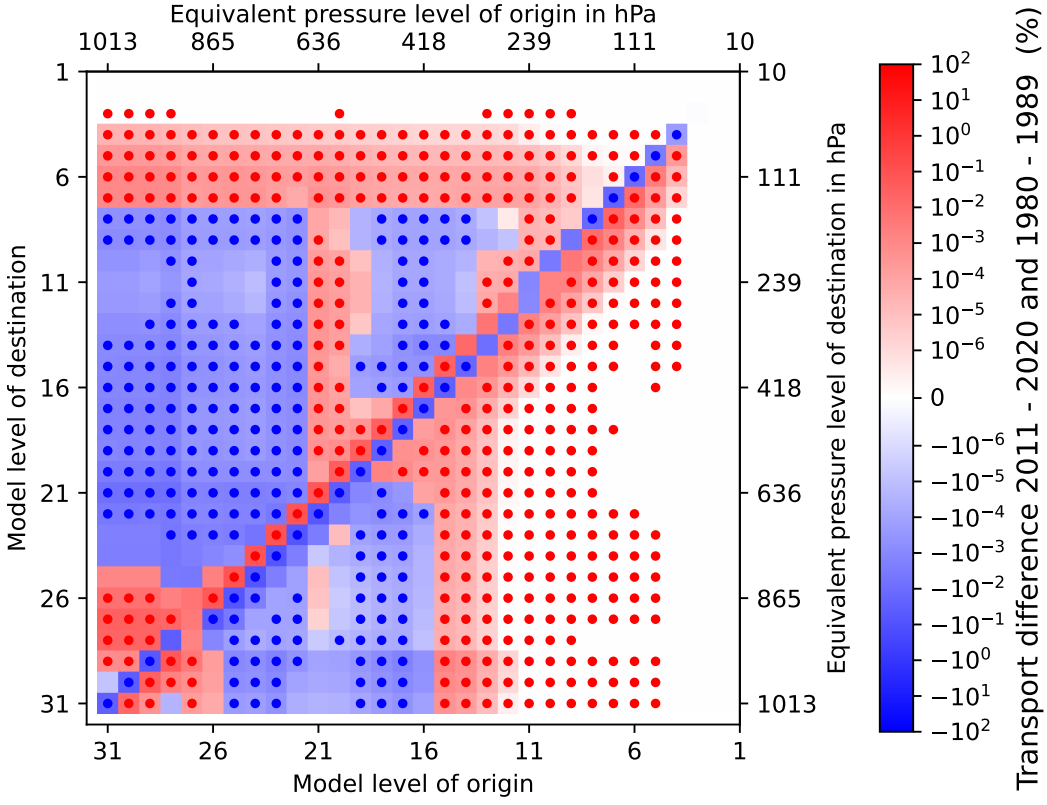

Figure 8. Changes in the convective mean transport in the tropics. Same as Fig. 5 but between 30°S and 30°N.

The differences in the time development are quite different when comparing the Northern hemisphere between 30°N and 60°N (Fig. 9) with the global picture. The upward transport is pronounced for a wide range of upper troposphere to lower stratospheric levels (levels 15 to 6) in the later time period in the mid-latitudes of the Northern hemisphere. This is related to the tropopause height in the extra-tropics. The tropopause height varies extensively between 30° and 60° and ranges from similar heights as in the tropics down below level 16.

https://doi.org/10.5194/egusphere-2025-293
Preprint. Discussion started: 18 February 2025

A similar picture is emerging for the Northern hemisphere and the global case keeping the difference in tropospheric ex-
315 pansion in mind. Less material is transported upward to a variety of height levels in the lower to upper troposphere (between level 30 and 16). The pattern is quite similar to the global case, but an increased transport to the lower troposphere (levels 26 to 28) becomes apparent when comparing the different decades globally which is not obvious on the Northern hemisphere. The changes in convective transport on the Northern hemisphere are similar in three other aspects to the trends on the global scale: (1) The downdrafts shift to higher origin levels. (2) Less air mass transport is ongoing in the lower levels from 2011 to 2020 in
320 comparison to 1980 to 1989. This is indicated by the positive changes in Fig. 9 on the main diagonal for a wide range of the lower and mid troposphere (levels 31 to 22). The transport increased above level 22 (mainly in the upper troposphere). (3) The large scale subsidence is enhanced in the upper levels.

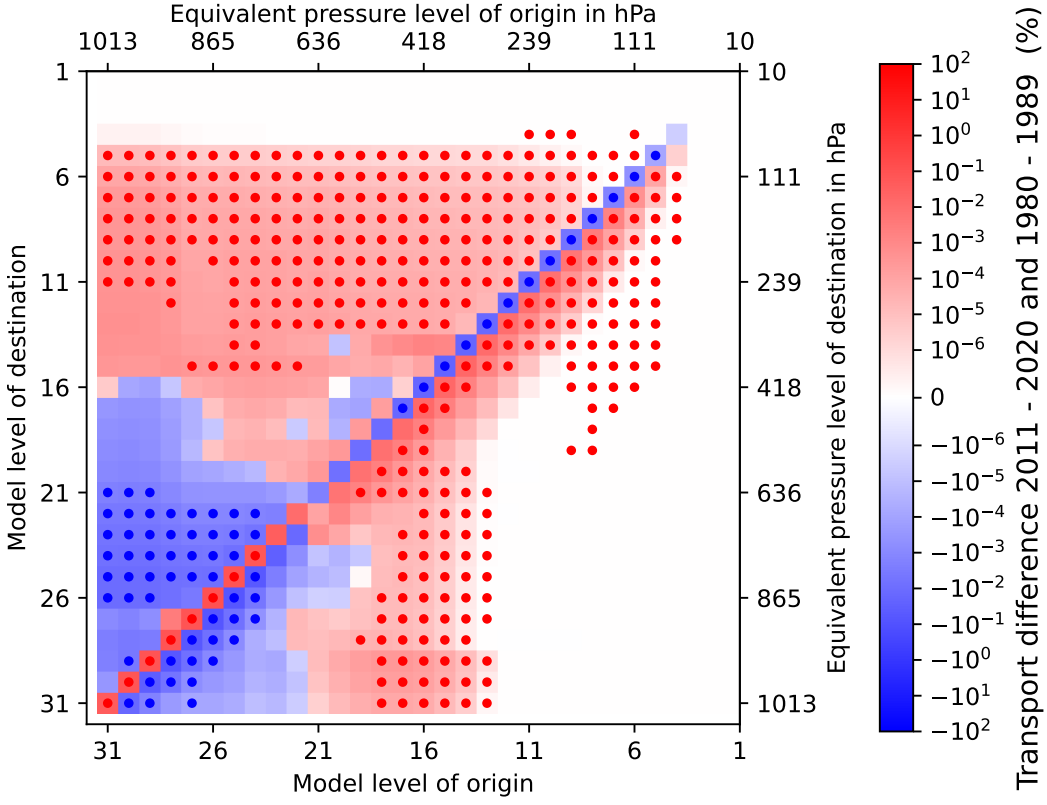

Figure 9. Northern hemispheric changes in the convective mean transport in the tropics. Same as Fig. 5 but for 60°N to 30°N.

The differences of the convective exchange matrix in the Southern hemisphere for the two time periods are shown in Fig. 10.
325 They are small when compared to the changes in the tropics and in the Northern hemispheric extra-tropics. Between 2011 and 2020 the convection tends to reach higher than in the reference period, but these changes are not statistically significant.

https://doi.org/10.5194/egusphere-2025-293
Preprint. Discussion started: 18 February 2025

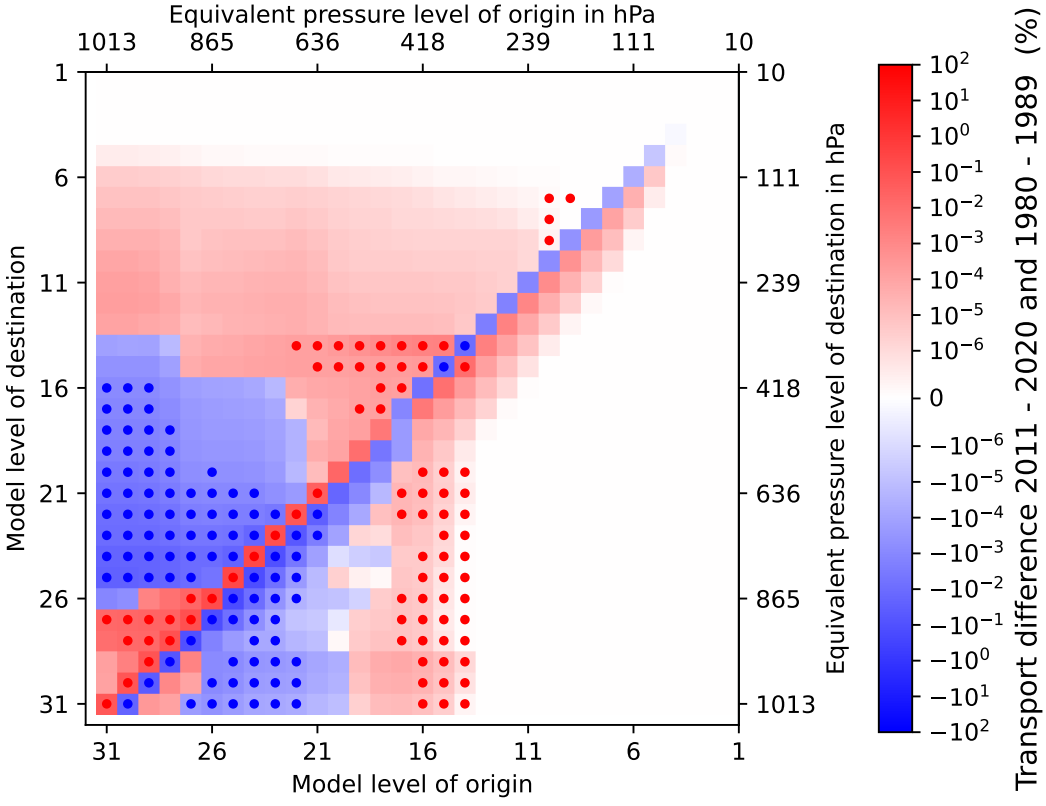

Figure 10. Southern hemispheric changes in the convective mean transport in the tropics. Same as Fig. 5 but for 60°S to 30°S.

The contrast between the changes on the Southern hemisphere and the Northern hemisphere can be attributed to the unequal distribution of land mass on both hemispheres, and therefore the lacking of intense continental mid-latitude convection.

Many transport processes changed although significantly in the levels below level 17 (mainly tropospheric levels). A shift of the downdrafts occurred qualitatively analogue to the global case (Fig. 5). The upward transport to the lower free troposphere (below level 26) increased and the transport of air originating at the same starting levels and reaching the levels 26 to 16 (mid to upper troposphere) is often significantly reduced. This is in good agreement with the findings on the global scale. It also supports that deep convection is suppressed more frequently in the later time period than in the reference period in the simulations.

We conclude that the Northern and Southern hemispheric changes are qualitatively compatible to the global and tropical changes taking the differences in the respective tropopause heights into account. However, the changes on the Southern hemisphere are not as significant as the ones on the Northern hemisphere and in the tropics.

https://doi.org/10.5194/egusphere-2025-293
Preprint. Discussion started: 18 February 2025

3.2.3 Regional differences

The vertical transport of air masses is strongly influenced by the location of the convective events. Therefore, the mean convective transport from the boundary layer (BL) to the upper troposphere (UT) is calculated for each grid column. The upper troposphere is heuristically defined as the region including the level of the tropopause down to the level where the pressure is equal to the tropopause pressure plus 150 hPa. The tropopause height and the height of the planetary boundary layer are taken directly from the EMAC output.

The mean upward transport is not directly comparable to a tracer concentration in the UT or tracer release studies as performed, e.g., by Levine et al. (2007); Hoyle et al. (2011) or Wang et al. (2021). Different processes interplay and impact the transport of a tracer. The convective exchange matrix opens the possibility to study the upward transport driven by convection undisturbed by other processes. In this section, the focus is on the regional differences and "trends" of the consecutively induced upward transport from the BL to the UT.

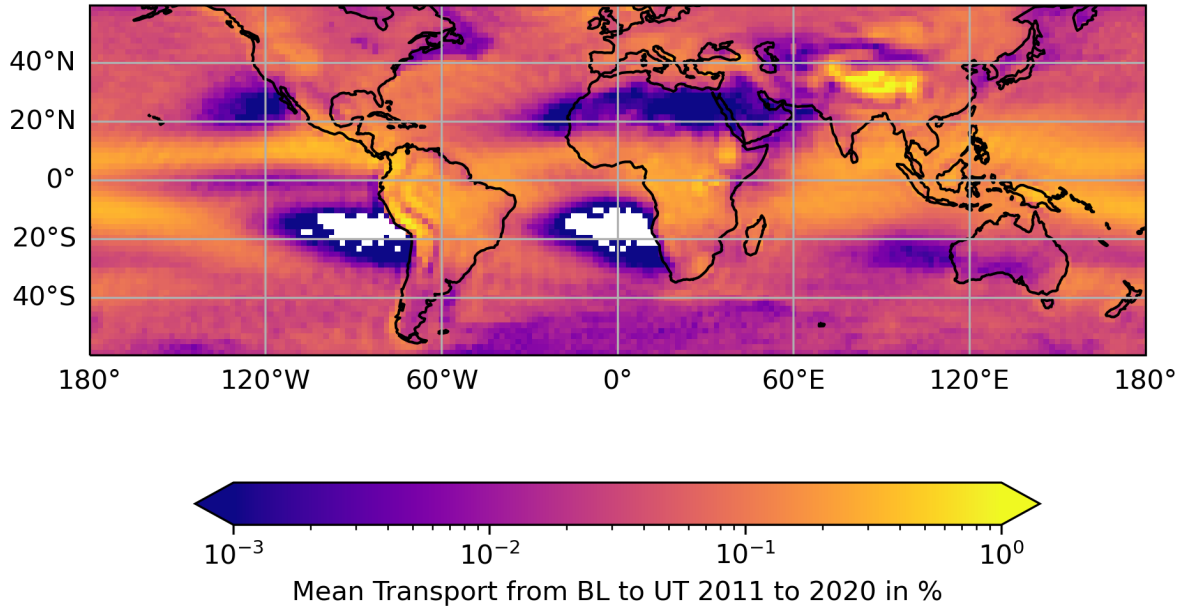

Figure 11. Ten year (2011 to 2020) mean convective mean transport from the planetary boundary layer height to upper troposphere within 12 min. The upper troposphere is defined as the region between the tropopause and the pressure height of tropopause plus 150 hPa.

The ten year mean of the BL to UT transport is shown in Fig. 11. The convective transport shows a similar structure as the convective precipitation (compare, e.g., Adler et al., 2017 and Sun et al., 2018, their Fig. 8) and the cloud top brightness temperature (compare Gettelman et al., 2002). The values are enhanced in the inner tropical convergence zone, Amazonia, central Africa and the North Atlantic storm track. No air masses were transported from the BL to the UT westerly of Africa

https://doi.org/10.5194/egusphere-2025-293
Preprint. Discussion started: 18 February 2025

and South America where subsidence is dominating the large-scale circulation patterns. Small but none zero values indicate very low (deep) convective activity westerly of Australia. This is also the case over North Africa and off the coast of California.

Particularly high portions of air mass were transported from the BL to the UT above the Himalaya and the North to central Andes mountains. This is for two reasons not surprising: (1) The model levels are compressed above high mountain areas. Thus, the distance between the BL and the UT decreases accordingly. (2) The precipitation rates calculated with the Tiedtke-Nordeng convection parameterisation within EMAC are to high compared to observations in these areas as shown by Tost et al. (2006) in their Fig. 2. It can therefore be assumed that the convective transport is as well overestimated based on the Tiedtke-Nordeng scheme in those regions.

The redistribution of air masses due to convection has changed significantly over the past decades as shown in Subsec. 3.2.1. However, the change in the mean BL to UT transport is characterised by regional differences (see Fig. 12). In dependence of the region the trend is either negative or positive.

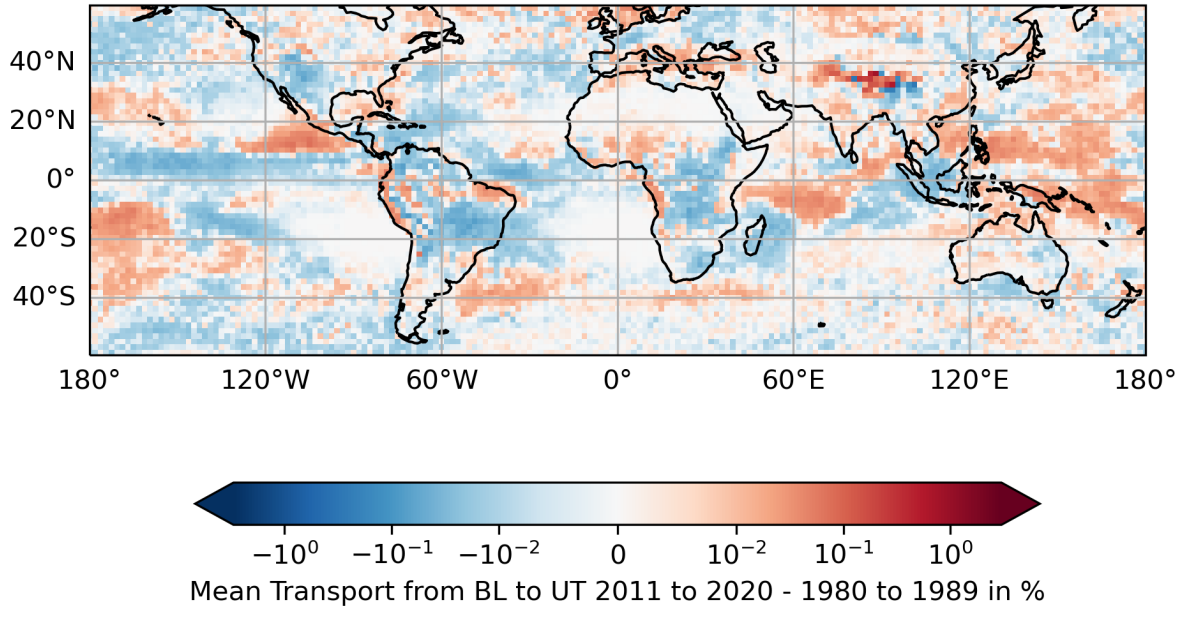

Figure 12. As Fig. 11 but for the difference of the mean values of 2011 to 2020 and 1980 to 1989.

Overall, the transport from BL to UT was only slightly smaller between 2011 to 2020 than in the reference period. The global (60°S to 60°N) area weighted average decreased from 0.07909% per time step (1980 to 1989) to 0.07829% per time step (2011 to 2020). This seems counter intuitive at first glance because of the significant increase of transported air masses to the upper levels of the convective exchange matrix (compare Fig. 5). First and foremost the increase of the convective outflow height leads to the increased transport to the levels 5 to 7 (in Fig. 5), likely due to an increase in the tropopause height. That does not necessarily imply an increased transport into the whole UT. The transport matrix shows instead that in many levels a larger portion of the air mass stays in the original level in the average between 2011 to 2020 as in the reference period.

https://doi.org/10.5194/egusphere-2025-293
Preprint. Discussion started: 18 February 2025

The mean transport from the BL to the tropopause region remains nearly unchanged. Thereby, the region of the tropopause is defined as the the level of the tropopause down to the level with a pressure equal to the pressure at the tropopause plus 50 hPa (in contrast to the UT, which was defined by the tropopause pressure + 150hPa). The mean transported portion was 0.02114% per time step in the reference period and increased marginally to 0.02118% per time step in 2011 to 2020. This indicates that less convection reaches the upper troposphere in general, but that the convective transport to the tropopause region stays similar due to compensating processes: The deeper penetration balances or even exceeds the effect due to the lower occurrence rate of deep convection. We note that these trends are rather small and need to be validated in the future.

The transport to the UT decreases close to the equator over the eastern Pacific. An increase becomes apparent North and partly also South of the equatorial region over the Eastern Atlantic. A possible weakening and widening of the Hadley cell (Lu et al., 2007; Hu et al., 2018) could explain this trend. In this framework, we cannot confirm or reject this hypothesis.

The problems of the underlying convection parameterisation is an important factor for the convective transport as well. The regions with the largest changes are widely the areas of the least accurate predictions of precipitation by the Tiedtke-Nordeng convection scheme. This convection parameterisation overestimates the precipitation at the pacific cost of Central America, Central Africa and the western Pacific and western Indian Ocean and underestimates the precipitation over the western Maritime continent as can bee seen in Fig. 2 by Tost et al. (2006). These areas show pronounced changes in the transport of BL air to the UT. These changes go therefore along with high uncertainties, which we cannot further quantify due to a lack of global observations of convective transport.

3.2.4 Natural variability in convective transport

To conclude whether the regional changes originate from climate change or are due to natural variability the intra-decadal variability is studied using extreme states. One El Niño event is compared to one La Niña event to investigate the maximal variability which can occur within one decade. For the El Niño event July 1st 1982 to June 30st 1983 was chosen because Ren et al. (2018) identified this event as an extreme El Niño event. According to Ren et al. (2018) a strong La Niña event took place in 1988 and 1989. This event is used for the analysis. For consistency reasons, we took the second half of 1988 and the first half of 1989 into account for the La Niña case.

The La Niña event (Fig. S4) has similar patterns as the ten year mean (Fig. 12). That was to be expected because La Niña is characterised by a strongly pronounced Walker circulation. In contrast, the direction of the circulation changes in the El Niño case (Fig. S5) leading to large differences in the convective transport patterns. These are especially large over the central Pacific. In the La Niña case, partly no deep convective transport was active at the equator in the considered time period. In contrast, BL to UT transport stands out during the El Niño event in exactly this region.

The mean transport to the UT from BL differs up to 0.38% per timestep in the area of the equator over the Pacific (Fig. 13). Sullivan et al. (2019) found an increased number of organised convective events in the same area comparing El Niño events with La Niña events between mid of 1983 and mid of 2008. This matches with the presented results from this study, that there is more transport into the UT from BL during the considered El Niño event. A huge decrease can be observed North and Southwards from the equator in the Pacific when comparing the El Niño event from 1982/83 with the La Niña event 1988/89

https://doi.org/10.5194/egusphere-2025-293
Preprint. Discussion started: 18 February 2025

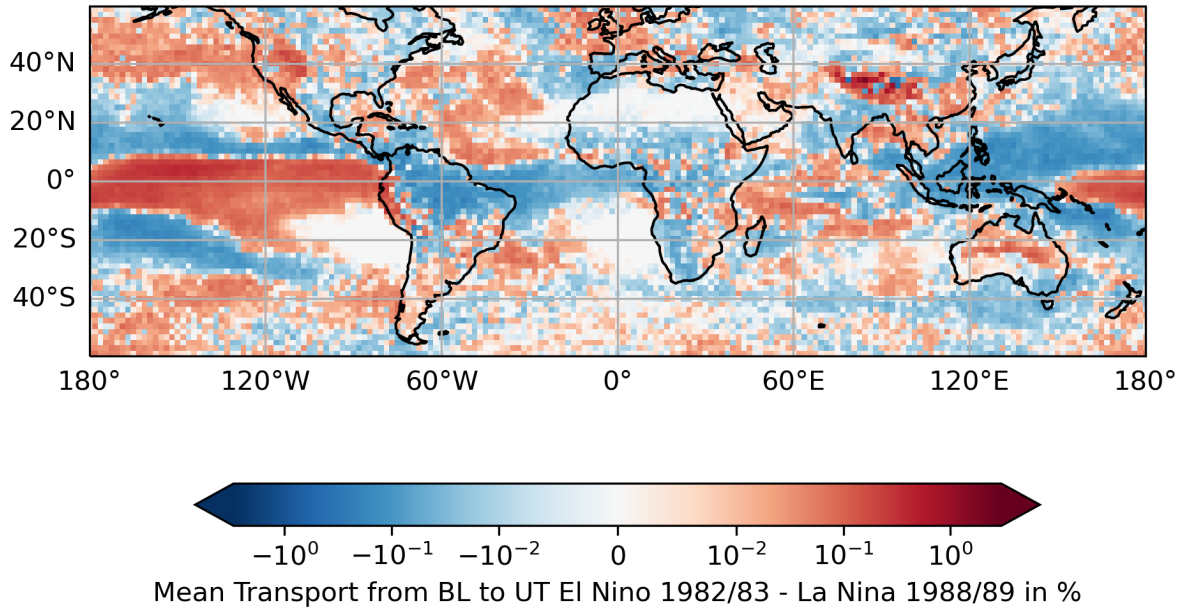

Figure 13. As Fig. 11 but for the difference between the el nino event 1982/83 and the la nina event 1988/89.

(see Fig. 13). The deep convective transport is also less active in the El Niño case over the maritime continent. This again is in good agreement with the findings of Sullivan et al. (2019) (their Figs. 3 and 4) concerning the occurrence of organised convection.

There are also huge differences over the equatorial Atlantic, the North-Western Atlantic and the Northern and Southern Pacific (Fig. 13). The differences in convective transport are striking when comparing the El Niño event with the La Niña event. They are much more pronounced than the differences which appear in the comparison of the ten year mean values (Fig. 12). Overall, there is no clear trend associated with the climate change in the convective BL to UT transport on regional scales, which exceeds the maximal variability within a decade.

4 Discussion

In Sec. 3.2.1, a rather small sample size is used to identify climate changes. To underline the significance of the global trend, we investigated also the time periods 1990 to 1999 and 2000 to 2009 and compared them to the reference period (Fig. S2 and Fig. S3) to further substantiate the discussed changes in the convectively induced redistribution of air masses. The time period 1990 to 1999 shows similar changes in the convective transport in comparison to the reference period from 1980 to 1989 as the latest considered time period. The trend is quantitatively much smaller but in terms of the qualitative changes comparably. The differences become more significant for the time period from 2000 to 2009 compared with the reference period. They are still

https://doi.org/10.5194/egusphere-2025-293
Preprint. Discussion started: 18 February 2025

not as pronounced as in Fig 5. Therefore, we conclude that the trend of the change is strengthening with time and is consistent over the decades with an increasing amplitude when the climate change signal intensifies.

The changes in the mean BL to UT transport are small in comparison to the maximal inner decadal variability on a regional scale in the past four decades. El Niño and La Niña events can lead to a huge natural variability of the regional convective transport efficiency within a decade. As a result, the trends in the background state appear partly masked by the high natural variability.

This study focuses on the representation of convective transport based on a convection parameterisation in an global circulation model. The Tiedtke-Nordeng convection parameterisation is based on basic physical principles, but is as all parameterisations a simplification of processes. Uncertainties arise from the use and the choice of each individual convection parameterisation. The convective transport differs for specific events when different convection parameterisations are used (Tost et al., 2010). We did not investigate how strongly the results of this study depend on the applied convection parameterisation. Therefore, this analysis can give an hint, how convection in general might behave but cannot provide any reliable information about the convective transport outside of the model framework of EMAC under the use of the Tiedtke-Nordeng convection scheme.

Furthermore, uncertainty arises due to the nudging because the ERA5 data already include convective processes. This might lead to less unstable conditions and therefore, might influence the triggering of convection in the model. This process was investigated in further detail by Schneider (2018). Schneider (2018) also discussed that the nudging also influences the tropopause height. Nudging is necessary to perform transient simulation as close as possible to the real world or at least to the reanalysis. Therefore, we can not avoid this issue. To test the robustness of our results, we performed another simulation where we only nudged the surface pressure, the sea surface temperature and the sea ice coverage. Furthermore, only climatologies were applied for the aerosol and green house gas forcing. The tropopause height is strongly affected in a quantitative sense. Nevertheless, neither the trend of the tropopause height nor the trends concerning the mean convective transport change qualitatively. We can therefore assume that influence of the nudging on the trends is minor.

Our results are to some extend consisted with other studies. An increase of the tropopause height / an decrease of the tropopause pressure has been already determined in several studies, for example, via radiosonde observations for the tropics by Seidel et al. (2001) and for the Northern hemisphere by Meng et al. (2021), via reanalysis data by Wilcox et al. (2012) and Weyland et al. (2024) (only for the Northern hemisphere) and by performing a mulitmodel intercomparison (Gettelman et al., 2010). Based on satellite data Richardson et al. (2022) and Raghuraman et al. (2024) observed an rising of the top height of high clouds in the tropics what gives us confidence with regard to the deeper convective clouds determined here. Also Muller et al. (2011) detected applying idealised simulations that convection reaches further with higher sea surface temperatures.

The trends in convection are still under discussion. Taszarek et al. (2021) discovered a wide-ranging decreasing trend in thunderstorm environments based on ERA5 data. Their calculated severe thunderstorm hours show a decrease for the mid latitudes, but partly an increase in the tropics. On the other hand Lepore et al. (2021) found an increasing trend for severe storms across various regions using proxies based on CIMP6 projections .

https://doi.org/10.5194/egusphere-2025-293
Preprint. Discussion started: 18 February 2025

Del Genio et al. (2007) found that the updraft speed can strengthen up to 1 m s^{-1} due to a CO_2 increase by a factor of two. Our simulations suggest a bimodal trend favouring no convective updrafts at all or stronger updraft mass fluxes (Fig. 6) from 2011 to 2020 compared to 1980 to 1989. Higher maximum values do not occur for the deep convective mass fluxes in our simulations. Del Genio et al. (2007) state that the updraft speed increased the most in the upper troposphere. This is in good agreement with our findings, that the deep updraft mass fluxes became stronger in the upper troposphere from 2011 to 2020 compared to the reference time period.

Stevenson et al. (2005) found in climate projections from 1990 to 2030 that tropical deep convection will reach higher and occur less often. The hindcast simulations from this study confirm these results. Though, in this study, the upraft strength increased for deep convective events in high altitude levels between 30° to 60° North and South in contrast to the results of Stevenson et al. (2005).

Furthermore, Gettelman et al. (2002) found a strong correlation of the deepest convection and the highest tropopause altitudes. However, they assumed based on the diurnal cycles of the tropopause height and the fractional area maximum of convection at lower temperatures as the colder point tropopause that the deep convection causes the colder and higher tropopause and not as supposed in this study the other way around. We cannot conclude with certainty whether there is a causality and which process is the result of the other and therefore, we agree with Gettelman et al. (2002) that further investigations are necessary.

5 Conclusions

We applied the submodule CVRANS, which handles the convective tracer transport in EMAC and can reproduce measured profiles of insoluble tracers (Tost et al., 2010), to investigate the changes in convective transport due to climate change. Thus, we take CVTRANS a step further (1) by establishing consistency with the underlying convection scheme (Tiedtke-Nordeng) concerning the turbulent detrainment and entrainment. (2) In addition, the entrained air into the downdraft can be directly detrain in the same level of the downdraft comparable to the proceed concerning the updraft. (1) and (2) contribute to a more realistic handling of the turbulent mixing associated with convection and give the opportunity to take the effects of turbulent mixing on the redistribution air masses driven by convection into account. (3) We implemented a new feature, the convective exchange matrix. That opens the path for a new analysis approach for convective transport by directly connecting the convective inflow and outflow levels. Thereby, convective transport can be investigated completely disentangled from the other processes.

Transient EMAC simulations have been performed using the updated CVTRANS for a 42 year time period. The convective exchange matrix has been applied to investigate changes in the convective transport due to recorded climate change. The convective transport reaches higher mainly due to an increase of the tropopause altitude.

In the extra-tropics, the upward transport increased to a wide range of high levels, across which the tropopause height shows substantial variability. However, the changes in the convective transport patterns are in general similar to the tropics. Respectively, less material is transported upward from the lower levels to levels between level 26 and 21 which can be associated with the free troposphere. This indicates that in total the convective transport is reduced in the extra-tropics. The same is the case in the tropics. Globally, this hypothesis is supported by the smaller mean transport from the BL to the UT from 2011 to 2020

https://doi.org/10.5194/egusphere-2025-293
Preprint. Discussion started: 18 February 2025

in comparison to the reference period. In fact, the simulations revealed a trend of decreasing occurrence of deep convection. Overall, this leads to less frequent but more penetrative convection which is in line with the results of Stevenson et al. (2005).

The goal of this study was to provide first insights in the adjustments of convective tracer transport to climate change. On global and zonal scale it becomes emerging that climate change open the path for higher but in total less upward transport of atmospheric tracers by deep convection leading in general to less transport from the BL to the UT. Furthermore, this study opens up new opportunities for the diagnosis of the impacts of convective transport on atmospheric tracers in chemistry climate simulations.

The regional trends are accompanied by great uncertainties. The extreme events associated with El Niño and La Niña lead to a large variability within a decade. This makes it hard to identify anthropogenically generated changes on a local scales. Lepore et al. (2021) had to deal also with large variability in the historical climate simulations and determined stronger signals using projections. Therefore, it might be promising to test how the convective transport will change in different climate projections but these test go far beyond the scope of this study. Moreover, the choice of convection parameterisation is a source of uncertainty which should be considered. More complex and comprehensive convection parameterisations exist nowadays. A overview of the developments can be found in Rio et al. (2019). For this reason, we plan to extend this study and investigate the impact of different convection parameterisations in the past and projected climate.

Code and data availability. The Modular Earth Submodel System (MESSy) is being continuously further developed and applied by a consortium of institutions. The usage of MESSy and access to the source code is licensed to all affiliates of institutions who are members of the MESSy Consortium. Institutions can become a member of the MESSy Consortium by signing the MESSy Memorandum of Understanding. More information can be found on the MESSy Consortium website (http://www.messy-interface.org). The code presented here was developed based on MESSy version 2.55.2 and is available in the developer branch of the model system and therefore also in the next official release. The data and the programme codes for the evaluation are available upon request.

https://doi.org/10.5194/egusphere-2025-293
Preprint. Discussion started: 18 February 2025

Author contributions. AJ and HT designed the study and developed the model code. With contributions from HT, AJ performed the simulations, analysed the data and wrote the paper.

Competing interests. The contact author has declared that none of the authors has any competing interests.

Acknowledgements. This research was partially founded by the Deutsche Forschungsgemeinschaft (DFG, German Research Foundation) – TRR 301 – Project-ID 428312742, The Tropopause Region in a Changing Atmosphere. AJ also thank Waves to Weather - the Transregional Collaborative Research Center (SFB/TRR165) for funding until June 2024. We acknowledge Mogon NHR computing system at Johannes Gutenberg-University Mainz and Levante at the German Climate Computing Centre (Deutsches Klimarechenzentrum) for the provided computing time and data disk space. We are grateful for the technical support at Mogon NHR computing system by Andreas Henkel and co-workers. We kindly appreciate Patrick Jöckel for his help concerning the MESSy setup and the code implementation within the MESSy framework. We thank Peter Hoor for some discussion. Many thanks to Cornelis Schwenk for his remarks especially with regard to the the reader's comprehensibility concerning the convective exchange matrix and the idea for Fig. S1.

https://doi.org/10.5194/egusphere-2025-293
Preprint. Discussion started: 18 February 2025

References

Adler, R. F., Gu, G., Sapiano, M., Wang, J.-J., and Huffman, G. J.: Global Precipitation: Means, Variations and Trends During the Satellite Era (1979–2014), Surveys in Geophysics, 38, 679–699, https://doi.org/10.1007/s10712-017-9416-4, 2017.

Bardakov, R., Krejci, R., Riipinen, I., and Ekman, A. M. L.: The Role of Convective Up- and Downdrafts in the Transport of Trace Gases in the Amazon, Journal of Geophysical Research: Atmospheres, 127, e2022JD037 265, https://doi.org/10.1029/2022JD037265, 2022.

Barth, M. C., Kim, S.-W., Wang, C., Pickering, K. E., Ott, L. E., Stenchikov, G., Leriche, M., Cautenet, S., Pinty, J.-P., Barthe, C., Mari, C., Helsdon, J. H., Farley, R. D., Fridlind, A. M., Ackerman, A. S., Spiridonov, V., and Telenta, B.: Cloud-scale model intercomparison of chemical constituent transport in deep convection, Atmospheric Chemistry and Physics, 7, 4709–4731, https://doi.org/10.5194/acp-7-4709-2007, 2007.

Bozem, H., Pozzer, A., Harder, H., Martinez, M., Williams, J., Lelieveld, J., and Fischer, H.: The influence of deep convection on HCHO and H_2O_2 in the upper troposphere over Europe, Atmospheric Chemistry and Physics, 17, 11 835–11 848, https://doi.org/10.5194/acp-17-11835-2017, 2017.

Cuchiara, G. C., Fried, A., Barth, M. C., Bela, M., Homeyer, C. R., Gaubert, B., Walega, J., Weibring, P., Richter, D., Wennberg, P., Crounse, J., Kim, M., Diskin, G., Hanisco, T. F., Wolfe, G. M., Beyersdorf, A., Peischl, J., Pollack, I. B., St. Clair, J. M., Woods, S., Tanelli, S., Bui, T. V., Dean-Day, J., Huey, L. G., and Heath, N.: Vertical Transport, Entrainment, and Scavenging Processes Affecting Trace Gases in a Modeled and Observed SEAC4RS Case Study, Journal of Geophysical Research: Atmospheres, 125, e2019JD031 957, https://doi.org/10.1029/2019JD031957, 2020.

Cuchiara, G. C., Fried, A., Barth, M. C., Bela, M. M., Homeyer, C. R., Walega, J., Weibring, P., Richter, D., Woods, S., Beyersdorf, A., Bui, T. V., and Dean-Day, J.: Effect of Marine and Land Convection on Wet Scavenging of Ozone Precursors Observed During a SEAC4RS Case Study, Journal of Geophysical Research: Atmospheres, 128, e2022JD037 107, https://doi.org/10.1029/2022JD037107, 2023.

Dagan, G., Koren, I., Altaratz, O., and Feingold, G.: Feedback mechanisms of shallow convective clouds in a warmer climate as demonstrated by changes in buoyancy, Environmental Research Letters, 13, 054 033, https://doi.org/10.1088/1748-9326/aac178, 2018.

Del Genio, A. D., Yao, M.-S., and Jonas, J.: Will moist convection be stronger in a warmer climate?, Geophysical Research Letters, 34, https://doi.org/10.1029/2007GL030525, 2007.

Doherty, R. M., Stevenson, D. S., Collins, W. J., and Sanderson, M. G.: Influence of convective transport on tropospheric ozone and its precursors in a chemistry-climate model, Atmospheric Chemistry and Physics, 5, 3205–3218, https://doi.org/10.5194/acp-5-3205-2005, 2005.

Emanuel, K. A.: Atmospheric convection, Oxford University Press, USA, 1994.

Eyring, V., Bony, S., Meehl, G. A., Senior, C. A., Stevens, B., Stouffer, R. J., and Taylor, K. E.: Overview of the Coupled Model Intercomparison Project Phase 6 (CMIP6) experimental design and organization, Geoscientific Model Development, 9, 1937–1958, https://doi.org/10.5194/gmd-9-1937-2016, 2016.

Feichter, J. and Crutzen, P. J.: Parameterization of vertical tracer transport due to deep cumulus convection in a global transport model and its evaluation with 222Radon measurements, Tellus B, 42, 100–117, https://doi.org/10.1034/j.1600-0889.1990.00011.x, 1990.

Frey, W., Schofield, R., Hoor, P., Kunkel, D., Ravegnani, F., Ulanovsky, A., Viciani, S., D'Amato, F., and Lane, T. P.: The impact of overshooting deep convection on local transport and mixing in the tropical upper troposphere/lower stratosphere (UTLS), Atmospheric Chemistry and Physics, 15, 6467–6486, https://doi.org/10.5194/acp-15-6467-2015, 2015.

https://doi.org/10.5194/egusphere-2025-293
Preprint. Discussion started: 18 February 2025

Gettelman, A., Salby, M. L., and Sassi, F.: Distribution and influence of convection in the tropical tropopause region, Journal of Geophysical Research: Atmospheres, 107, ACL 6–1–ACL 6–12, https://doi.org/10.1029/2001JD001048, 2002.

Gettelman, A., Hegglin, M. I., Son, S.-W., Kim, J., Fujiwara, M., Birner, T., Kremser, S., Rex, M., Añel, J. A., Akiyoshi, H., Austin, J., Bekki, S., Braesike, P., Brühl, C., Butchart, N., Chipperfield, M., Dameris, M., Dhomse, S., Garny, H., Hardiman, S. C., Jöckel, P., Kinnison, D. E., Lamarque, J. F., Mancini, E., Marchand, M., Michou, M., Morgenstern, O., Pawson, S., Pitari, G., Plummer, D., Pyle, J. A., Rozanov, E., Scinocca, J., Shepherd, T. G., Shibata, K., Smale, D., Teyssèdre, H., and Tian, W.: Multimodel assessment of the upper troposphere and lower stratosphere: Tropics and global trends, Journal of Geophysical Research: Atmospheres, 115, https://doi.org/10.1029/2009JD013638, 2010.

Gordon, A. E., Homeyer, C. R., Smith, J. B., Ueyama, R., Dean-Day, J. M., Atlas, E. L., Smith, K., Pittman, J. V., Sayres, D. S., Wilmouth, D. M., Pandey, A., St. Clair, J. M., Hanisco, T. F., Hare, J., Hannun, R. A., Wofsy, S., Daube, B. C., and Donnelly, S.: Airborne observations of upper troposphere and lower stratosphere composition change in active convection producing above-anvil cirrus plumes, Atmospheric Chemistry and Physics, 24, 7591–7608, https://doi.org/10.5194/acp-24-7591-2024, 2024.

Hersbach, H., Bell, B., Berrisford, P., Hirahara, S., Horányi, A., Muñoz-Sabater, J., Nicolas, J., Peubey, C., Radu, R., Schepers, D., Simmons, A., Soci, C., Abdalla, S., Abellan, X., Balsamo, G., Bechtold, P., Biavati, G., Bidlot, J., Bonavita, M., De Chiara, G., Dahlgren, P., Dee, D., Diamantakis, M., Dragani, R., Flemming, J., Forbes, R., Fuentes, M., Geer, A., Haimberger, L., Healy, S., Hogan, R. J., Hólm, E., Janisková, M., Keeley, S., Laloyaux, P., Lopez, P., Lupu, C., Radnoti, G., de Rosnay, P., Rozum, I., Vamborg, F., Villaume, S., and Thépaut, J.-N.: The ERA5 global reanalysis, Quarterly Journal of the Royal Meteorological Society, 146, 1999–2049, https://doi.org/10.1002/qj.3803, 2020.

Hoyle, C. R., Marécal, V., Russo, M. R., Allen, G., Arteta, J., Chemel, C., Chipperfield, M. P., D'Amato, F., Dessens, O., Feng, W., Hamilton, J. F., Harris, N. R. P., Hosking, J. S., Lewis, A. C., Morgenstern, O., Peter, T., Pyle, J. A., Reddmann, T., Richards, N. A. D., Telford, P. J., Tian, W., Viciani, S., Volz-Thomas, A., Wild, O., Yang, X., and Zeng, G.: Representation of tropical deep convection in atmospheric models – Part 2: Tracer transport, Atmospheric Chemistry and Physics, 11, 8103–8131, https://doi.org/10.5194/acp-11-8103-2011, 2011.

Hu, Y., Huang, H., and Zhou, C.: Widening and weakening of the Hadley circulation under global warming, Science Bulletin, 63, 640–644, https://doi.org/10.1016/j.scib.2018.04.020, 2018.

Jeuken, A. B. M., Siegmund, P. C., Heijboer, L. C., Feichter, J., and Bengtsson, L.: On the potential of assimilating meteorological analyses in a global climate model for the purpose of model validation, Journal of Geophysical Research: Atmospheres, 101, 16 939–16 950, https://doi.org/https://doi.org/10.1029/96JD01218, 1996.

Jöckel, P.: Technical note: Recursive rediscretisation of geo-scientific data in the Modular Earth Submodel System (MESSy), Atmospheric Chemistry and Physics, 6, 3557–3562, https://doi.org/10.5194/acp-6-3557-2006, 2006.

Jöckel, P., Tost, H., Pozzer, A., Brühl, C., Buchholz, J., Ganzeveld, L., Hoor, P., Kerkweg, A., Lawrence, M. G., Sander, R., Steil, B., Stiller, G., Tanarhte, M., Taraborrelli, D., van Aardenne, J., and Lelieveld, J.: The atmospheric chemistry general circulation model ECHAM5/MESSy1: consistent simulation of ozone from the surface to the mesosphere, Atmospheric Chemistry and Physics, 6, 5067–5104, https://doi.org/10.5194/acp-6-5067-2006, 2006.

Jöckel, P., Kerkweg, A., Pozzer, A., Sander, R., Tost, H., Riede, H., Baumgaertner, A., Gromov, S., and Kern, B.: Development cycle 2 of the Modular Earth Submodel System (MESSy2), Geoscientific Model Development, 3, 717–752, https://doi.org/10.5194/gmd-3-717-2010, 2010.

Jöckel, P., Tost, H., Pozzer, A., Kunze, M., Kirner, O., Brenninkmeijer, C. A. M., Brinkop, S., Cai, D. S., Dyroff, C., Eckstein, J., Frank, F., Garny, H., Gottschaldt, K.-D., Graf, P., Grewe, V., Kerkweg, A., Kern, B., Matthes, S., Mertens, M., Meul, S., Neumaier, M., Nützel,

https://doi.org/10.5194/egusphere-2025-293
Preprint. Discussion started: 18 February 2025

M., Oberländer-Hayn, S., Ruhnke, R., Runde, T., Sander, R., Scharffe, D., and Zahn, A.: Earth System Chemistry integrated Modelling (ESCiMo) with the Modular Earth Submodel System (MESSy) version 2.51, Geoscientific Model Development, 9, 1153–1200, https://doi.org/10.5194/gmd-9-1153-2016, 2016.

Lawrence, M. G. and Rasch, P. J.: Tracer Transport in Deep Convective Updrafts: Plume Ensemble versus Bulk Formulations, Journal of the Atmospheric Sciences, 62, 2880 – 2894, https://doi.org/10.1175/JAS3505.1, 2005.

Lawrence, M. G. and Salzmann, M.: On interpreting studies of tracer transport by deep cumulus convection and its effects on atmospheric chemistry, Atmospheric Chemistry and Physics, 8, 6037–6050, https://doi.org/10.5194/acp-8-6037-2008, 2008.

Lawrence, M. G., von Kuhlmann, R., Salzmann, M., and Rasch, P. J.: The balance of effects of deep convective mixing on tropospheric ozone, Geophysical Research Letters, 30, https://doi.org/10.1029/2003GL017644, 2003.

Lepore, C., Abernathey, R., Henderson, N., Allen, J. T., and Tippett, M. K.: Future Global Convective Environments in CMIP6 Models, Earth's Future, 9, e2021EF002 277, https://doi.org/10.1029/2021EF002277, 2021.

Levine, J. G., Braesicke, P., Harris, N. R. P., Savage, N. H., and Pyle, J. A.: Pathways and timescales for troposphere-to-stratosphere transport via the tropical tropopause layer and their relevance for very short lived substances, Journal of Geophysical Research: Atmospheres, 112, https://doi.org/10.1029/2005JD006940, 2007.

Li, Y., Pickering, K. E., Barth, M. C., Bela, M. M., Cummings, K. A., and Allen, D. J.: Evaluation of Parameterized Convective Transport of Trace Gases in Simulation of Storms Observed During the DC3 Field Campaign, Journal of Geophysical Research: Atmospheres, 123, 11,238–11,261, https://doi.org/10.1029/2018JD028779, 2018.

Lu, J., Vecchi, G. A., and Reichler, T.: Expansion of the Hadley cell under global warming, Geophysical Research Letters, 34, https://doi.org/10.1029/2006GL028443, 2007.

Mahowald, N. M., Rasch, P. J., and Prinn, R. G.: Cumulus parameterizations in chemical transport models, Journal of Geophysical Research: Atmospheres, 100, 26 173–26 189, 1995.

Mari, C., Jacob, D. J., and Bechtold, P.: Transport and scavenging of soluble gases in a deep convective cloud, Journal of Geophysical Research: Atmospheres, 105, 22 255–22 267, https://doi.org/10.1029/2000JD900211, 2000.

Meng, L., Liu, J., Tarasick, D. W., Randel, W. J., Steiner, A. K., Wilhelmsen, H., Wang, L., and Haimberger, L.: Continuous rise of the tropopause in the Northern Hemisphere over 1980–2020, Science Advances, 7, eabi8065, https://doi.org/10.1126/sciadv.abi8065, 2021.

Muller, C. J., O'Gorman, P. A., and Back, L. E.: Intensification of Precipitation Extremes with Warming in a Cloud-Resolving Model, Journal of Climate, 24, 2784 – 2800, https://doi.org/10.1175/2011JCLI3876.1, 2011.

Nordeng, T.-E.: Extended versions of the convective parametrization scheme at ECMWF and their impact on the mean and transient activity of the model in the tropics, ECMWF Technical Memoranda, pp. 1–41, https://doi.org/10.21957/e34xwhysw, 1994.

Ouwersloot, H. G., Pozzer, A., Steil, B., Tost, H., and Lelieveld, J.: Revision of the convective transport module CVTRANS 2.4 in the EMAC atmospheric chemistry–climate model, Geoscientific Model Development, 8, 2435–2445, https://doi.org/10.5194/gmd-8-2435-2015, 2015.

Raghuraman, S. P., Medeiros, B., and Gettelman, A.: Observational Quantification of Tropical High Cloud Changes and Feedbacks, Journal of Geophysical Research: Atmospheres, 129, e2023JD039 364, https://doi.org/10.1029/2023JD039364, 2024.

Ray, E. A., Rosenlof, K. H., Richard, E. C., Hudson, P. K., Cziczo, D. J., Loewenstein, M., Jost, H.-J., Lopez, J., Ridley, B., Weinheimer, A., Montzka, D., Knapp, D., Wofsy, S. C., Daube, B. C., Gerbig, C., Xueref, I., and Herman, R. L.: Evidence of the effect of summertime midlatitude convection on the subtropical lower stratosphere from CRYSTAL-FACE tracer measurements, Journal of Geophysical Research: Atmospheres, 109, https://doi.org/10.1029/2004JD004655, 2004.

https://doi.org/10.5194/egusphere-2025-293
Preprint. Discussion started: 18 February 2025

Ren, H.-L., Lu, B., Wan, J., Tian, B., and Zhang, P.: Identification standard for ENSO events and its application to climate monitoring and prediction in China, Journal of Meteorological Research, 32, 923–936, https://doi.org/10.1007/s13351-018-8078-6, 2018.

Revell, L. E., Stenke, A., Luo, B., Kremser, S., Rozanov, E., Sukhodolov, T., and Peter, T.: Impacts of Mt Pinatubo volcanic aerosol on the tropical stratosphere in chemistry–climate model simulations using

640 CCMI and CMIP6 stratospheric aerosol data, Atmospheric Chemistry and Physics, 17, 13 139–13 150, https://doi.org/10.5194/acp-17-13139-2017, 2017.

Richardson, M. T., Roy, R. J., and Lebsock, M. D.: Satellites Suggest Rising Tropical High Cloud Altitude: 2002–2021, Geophysical Research Letters, 49, e2022GL098 160, https://doi.org/10.1029/2022GL098160, 2022.

Rio, C., Del Genio, A. D., and Hourdin, F.: Ongoing breakthroughs in convective parameterization, Current Climate Change Reports, 5,

645 95–111, https://doi.org/10.1007/s40641-019-00127-w, 2019.

Roeckner, E., Brokopf, R., Esch, M., Giorgetta, M., Hagemann, S., Kornblueh, L., Manzini, E., Schlese, U., and Schulzweida, U.: Sensitivity of Simulated Climate to Horizontal and Vertical Resolution in the ECHAM5 Atmosphere Model, Journal of Climate, 19, 3771 – 3791, https://doi.org/10.1175/JCLI3824.1, 2006.

Schneider, S.: Simulation of a Permian climate and analysis of atmospheric transport and mixing processes, Mainz, Germany, Dissertation,

650 2018.

Seidel, D. J., Ross, R. J., Angell, J. K., and Reid, G. C.: Climatological characteristics of the tropical tropopause as revealed by radiosondes, Journal of Geophysical Research: Atmospheres, 106, 7857–7878, https://doi.org/10.1029/2000JD900837, 2001.

Stevenson, D., Doherty, R., Sanderson, M., Johnson, C., Collins, B., and Derwent, D.: Impacts of climate change and variability on tropospheric ozone and its precursors, Faraday Discuss., 130, 41–57, https://doi.org/10.1039/B417412G, 2005.

655 Sullivan, S. C., Schiro, K. A., Stubenrauch, C., and Gentine, P.: The Response of Tropical Organized Convection to El Niño Warming, Journal of Geophysical Research: Atmospheres, 124, 8481–8500, https://doi.org/10.1029/2019JD031026, 2019.

Sun, Q., Miao, C., Duan, Q., Ashouri, H., Sorooshian, S., and Hsu, K.-L.: A Review of Global Precipitation Data Sets: Data Sources, Estimation, and Intercomparisons, Reviews of Geophysics, 56, 79–107, https://doi.org/10.1002/2017RG000574, 2018.

Tanre, D., Geleyn, J., and Slingo, J.: First results of the introduction of an advanced aerosol-radiation interaction in the ECMWF low

660 resolution global model, in: Aerosols and their climatic effects, edited by Gerber, H. and Deepak, A., pp. 133 – 177, A. Deepak Hampton, Va., Meeting of Experts on Aerosols and their climatic effects, Williamsburg, Virginia, 28–30 March 1983, 1984.

Taszarek, M., Allen, J. T., Marchio, M., and Brooks, H. E.: Global climatology and trends in convective environments from ERA5 and rawinsonde data, NPJ climate and atmospheric science, 4, 35, https://doi.org/10.1038/s41612-021-00190-x, 2021.

Tiedtke, M.: A Comprehensive Mass Flux Scheme for Cumulus Parameterization in Large-Scale Models, Monthly Weather Review, 117,

665 1779 – 1800, https://doi.org/10.1175/1520-0493(1989)117<1779:ACMFSF>2.0.CO;2, 1989.

Tinney, E. N. and Homeyer, C. R.: A 13-year Trajectory-Based Analysis of Convection-Driven Changes in Upper Troposphere Lower Stratosphere Composition Over the United States, Journal of Geophysical Research: Atmospheres, 126, e2020JD033 657, https://doi.org/10.1029/2020JD033657, 2021.

Tost, H., Jöckel, P., and Lelieveld, J.: Influence of different convection parameterisations in a GCM, Atmospheric Chemistry and Physics, 6,

670 5475–5493, https://doi.org/10.5194/acp-6-5475-2006, 2006.

Tost, H., Lawrence, M. G., Brühl, C., Jöckel, P., Team, T. G., and Team, T. S.-O.-D.: Uncertainties in atmospheric chemistry modelling due to convection parameterisations and subsequent scavenging, Atmospheric Chemistry and Physics, 10, 1931–1951, https://doi.org/10.5194/acp-10-1931-2010, 2010.

https://doi.org/10.5194/egusphere-2025-293
Preprint. Discussion started: 18 February 2025

Vella, R., Forrest, M., Lelieveld, J., and Tost, H.: Isoprene and monoterpene simulations using the chemistry–climate model EMAC (v2.55) with interactive vegetation from LPJ-GUESS (v4.0), Geoscientific Model Development, 16, 885–906, https://doi.org/10.5194/gmd-16-885-2023, 2023.

Wang, X., Randel, W., and Wu, Y.: Infrequent, Rapid Transport Pathways to the Summer North American Upper Troposphere and Lower Stratosphere, Geophysical Research Letters, 48, e2020GL089 763, https://doi.org/10.1029/2020GL089763, 2021.

Weyland, F., Hoor, P., Kunkel, D., Birner, T., Plöger, F., and Turhal, K.: Long-term changes in the thermodynamic structure of the lowermost stratosphere inferred from ERA5 reanalysis data, EGUsphere [preprint], pp. 1–26, https://doi.org/10.5194/egusphere-2024-1700, 2024.

Wilcox, L. J., Hoskins, B. J., and Shine, K. P.: A global blended tropopause based on ERA data. Part II: Trends and tropical broadening, Quarterly Journal of the Royal Meteorological Society, 138, 576–584, https://doi.org/10.1002/qj.910, 2012.

Winterstein, F. and Jöckel, P.: Methane chemistry in a nutshell – the new submodels CH4 (v1.0) and TRSYNC (v1.0) in MESSy (v2.54.0), Geoscientific Model Development, 14, 661–674, https://doi.org/10.5194/gmd-14-661-2021, 2021.

Wu, X., Fu, Q., and Kodama, C.: Response of Tropical Overshooting Deep Convection to Global Warming Based on Global Cloud-Resolving Model Simulations, Geophysical Research Letters, 50, e2023GL104 210, https://doi.org/10.1029/2023GL104210, e2023GL104210 2023GL104210, 2023.